CrossMark

ORIGINAL PAPER

Rock Drilling Performance Evaluation by an Energy Dissipation Based Rock Brittleness Index

H. Munoz[1,2] · A. Taheri[2] · E. K. Chanda[2]

Abstract To reliably estimate drilling performance both tool–rock interaction laws along with a proper rock brittleness index are required to be implemented. In this study, the performance of a single polycrystalline diamond compact (PDC) cutter cutting and different drilling methods including PDC rotary drilling, roller-cone rotary drilling and percussive drilling were investigated. To investigate drilling performance by rock strength properties, laboratory PDC cutting tests were performed on different rocks to obtain cutting parameters. In addition, results of laboratory and field drilling on different rocks found elsewhere in literature were used. Laboratory and field cutting and drilling test results were coupled with values of a new rock brittleness index proposed herein and developed based on energy dissipation withdrawn from the complete stress–strain curve in uniaxial compression. To quantify cutting and drilling performance, the intrinsic specific energy in rotary-cutting action, i.e. the energy consumed in pure cutting action, and drilling penetration rate values in percussive action were used. The results show that the new energy-based brittleness index successfully describes the performance of different cutting and drilling methods and therefore is relevant to assess drilling performance for engineering applications.

1 Introduction

Rock drilling is an essential task in mining engineering and deep exploration industry. In this sense, drilling performance is one of the most important parameters to take into account when evaluating project feasibility and economy. Equipment type and specifications is strongly dependent on predicting the performance of the cutting tool in the field. In this sense, several attempts have been made to assess drilling performance by correlating different rock mechanical and physical properties with the drilling penetration rate. For instance, unconfined compressive strength (UCS) has been determined as the dominant rock property in penetration rate prediction for rotary drills (Kahraman 1999) and among rock properties, uniaxial compressive strength, Brazilian tensile strength, point load strength and Schmidt hammer value have been determined as the dominant rock properties affecting the penetration rate of percussive drills (Kahraman et al. 2003). In this same manner, force-indentation curves of indentation tests have been deemed relevant develop a drillability index for the prediction of penetration rates of rotary blast-hole drills and rock formations mechanical and physical properties (Kahraman et al. 2000). Furthermore, rock texture, grain size, density, P-wave velocity, unconfined compressive strength, Mohs hardness and rock mass structural parameters have been used to build a number of drillability indices (Altindag 2003, 2009; Hoseinie et al. 2008; Taheri et al. 2016).

✉ H. Munoz
  henry.munozprincipe@adelaide.edu.au

1 Deep Exploration Technologies Cooperative Research Centre DET CRC, Export Park, Adelaide, SA 5950, Australia

2 School of Civil, Environmental and Mining Engineering, The University of Adelaide, North Terrace, Adelaide, SA 5005, Australia

A generalised method to relate drilling performance with rock strength characteristics has not been developed yet. This is due to the complexity of interactions among the variables involved in the drilling process encompassing not only rock properties, but also the nature of drilling. Therefore, not only rock properties, but also different sets of drilling forces acting on rock as well as drilling method all have impacts on the drilling performance (Detournay and Defourny 1992; Detournay et al. 2008; Franca 2010, 2011; Franca et al. 2015; Hustrulid and Fairhurst 1971b; Teale 1965). In this view, by coupling relevant drilling parameters with relevant rock properties, a reliable drilling performance prediction method can be developed.

On one hand, to predict rock drilling performance and optimisation of drilling operation, tool–rock interaction laws, i.e. the relations between forces acting on the tool in contact with rock, are essential (Detournay and Defourny 1992; Detournay et al. 2008; Franca 2010, 2011; Franca et al. 2015; Hustrulid and Fairhurst 1971a, b, 1972a, b). For instance, through tool–rock interaction laws, it was found that during rotary drilling, the specific energy (SE), the work done to excavate a unit volume of rock (Teale 1965), accounts for both energy consumed in rock cutting and energy consumed in friction between the tool and the rock (Detournay and Defourny 1992; Teale 1965). In this instance, the energy consumed in pure cutting action of rock is measured by the intrinsic specific energy (ε) attainable at the cutting point (Detournay and Defourny 1992; Detournay et al. 2008; Franca 2010; Franca et al. 2015). The intrinsic specific energy quantifies the maximum cutting efficiency associated with the optimum cutting force and its magnitude depends on the nature of the rock (Detournay and Defourny 1992; Teale 1965), the surrounding pressure on the rock (Detournay and Atkinson 2000) and the drilling technique being used (Detournay et al. 2008; Franca 2010; Franca et al. 2015). In the case of percussive drilling, tool–rock interactions are focused mostly in the prediction of the penetration rate and the optimum thrust. Experimental results with wedge-shaped cutter percussive bits show that tool–rock interaction can be simulated by linear relationships in an idealised force–penetration curve for percussive action and percussive penetration rate (Franca 2011; Hustrulid and Fairhurst 1971a, b, 1972a, b).

On the other hand, rock brittleness is a concept yet to be investigated as there is not a unique criterion able to describe rock brittleness quantitatively nor consensus about the most suitable and reliable brittleness index to apply to different rock engineering works encountered in the field. For instance, previously a number of different criteria to assess rock brittleness have been developed upon pre-peak stress–strain characteristics in uniaxial compression experiments including ratios between elastic to plastic strain (Hucka and Das 1974) as well as strain-energy relations (Hucka and Das 1974; Kidybiński 1981). However, those criteria are insufficient in order to describe unambiguously a scale of brittleness to ductility of rock (Munoz et al. 2016; Tarasov and Potvin 2013; Tarasov and Randolph 2011). In the same manner, some brittleness indices which are defined upon rock compressive strength, UCS, and tensile strength, TS (Altindag 2002; Hucka and Das 1974; Kahraman 2002), cannot describe a scale of brittleness to ductility of rock (Tarasov and Potvin 2013). This is mainly because, rock failure behaviour cannot be described by a ratio between compressive and tensile strength and, generally, compressive and tensile strength can be obtained from each other. In addition, those brittleness indices cannot correlate well with the rock compressive strength. Figure 1 shows uniaxial compressive-to-tensile-strength brittleness indices defined as B_1 (Altindag 2002), B_2 (Hucka and Das 1974) and B_3 (Altindag 2002), see expressions below, plotted against the respective rock uniaxial compressive strength values. In this figure, data found in the literature elsewhere (Howarth 1987; Paone et al. 1969; Schmidt 1972; Selim and Bruce 1970) is plotted.

$$B_1 = \frac{\text{UCS}}{\text{TS}} \tag{1}$$

$$B_2 = \frac{\text{UCS} - \text{TS}}{\text{UCS} + \text{TS}} \tag{2}$$

$$B_3 = \frac{\text{UCS} \times \text{TS}}{2} [\text{MPa} \times \text{MPa}] \tag{3}$$

As it may be seen in Fig. 1, in general, brittleness indices, B_1 and B_2 are not able to describe a scale of brittleness with rock compressive strength increasing, i.e. a soft rock may have the same brittleness B_1 and B_2 as a hard rock. Thus, if B_1 and B_2 are used to assess drilling performance of either rotary or percussive drilling, it can be expected to obtained no sound relationships between B_1 and B_2 and drilling parameters for instance the drilling penetration rate, as demonstrated in previous studies (Altindag 2009, 2010). Although B_3 shows a better correlation with the drilling penetration rate (Altindag 2009, 2010), the foundation of brittleness B_3 gives conflicting results to describe rock brittle to ductile scale (Tarasov and Potvin 2013).

The discussion presented above, demonstrated that in order to predict drilling performance successfully, first tool–rock interaction laws should be implemented to quantify drilling. In this respect, it was found that there are very few studies that consider tool–rock interaction to characterise drilling performance. Second, a proper brittleness index is required to describe rock failure characteristics in drilling. As a result, the present study aims at
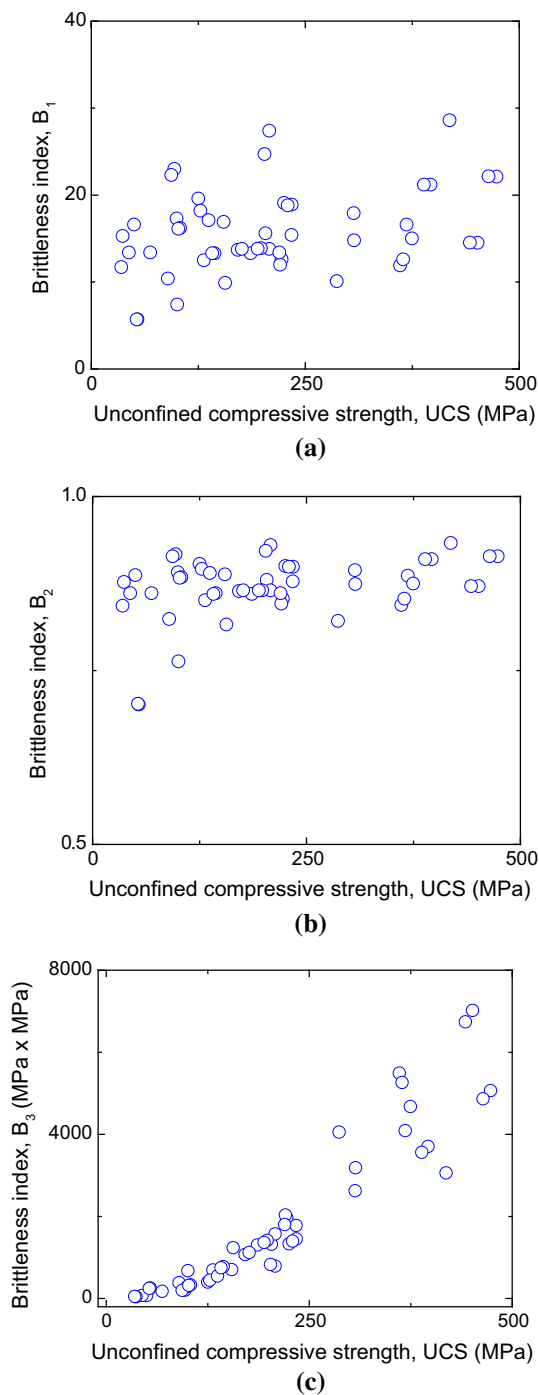
Fig. 1 Relations between compressive-to-tensile brittleness indices **a** B_1, **b** B_2 and **c** B_3 with unconfined compressive strength. Data from literature (Howarth 1987; Paone et al. 1969; Schmidt 1972; Selim and Bruce 1970)

evaluating drilling performance by taking into account both the drilling response from tool–rock interaction laws and by defining a new energy-based rock brittleness index that considers rock failure behaviour which is able to describe an ambiguous brittleness scale from ductile to brittle.

In this study, the performance of two major mechanical drilling methods, namely rotary drilling and percussive drilling, are investigated against rock brittleness capacity by the new energy-based brittleness index. The intrinsic specific energy and rate of penetration, as two main drilling performance parameters, were coupled with rock brittleness. To validate this proposal, cutting experiments with a single PDC cutter were carried out on different rock types. In addition, independent rotary drilling as well as percussive drilling results from laboratory and field tests from the literature were used.

2 New Energy-Based Brittleness Index

A recently developed brittleness index by Munoz et al. (2016) upon fracture strain-energy quantities withdrawn from the area under complete stress–strain curve of rocks in uniaxial compressive tests is proposed herein to study drilling performance by rock brittleness capacity. This brittleness index takes into account post-peak instability in uniaxial compression as post-peak instability of rock during compression can be treated as a manifestation of rock brittleness (Tarasov and Randolph 2011). That is, an increase in the post-peak energy indicates an increase of stability (i.e. a decrease in brittleness). In the same manner, a dramatic decrease of post-peak energy indicates less stability of the failure process (i.e. an increase in brittleness). Pre-peak and post-peak energy relations are the basis of the proposed brittleness index. Pre-peak energy is considered to dissipate due to micro cracking during the loading process up to the peak (Jansen and Edwin 1995; Jansen and Shah 1997). On the other hand, energy dissipated in post-peak regime represents that energy dissipated during coalescence of micro fractures initiated before peak stress and energy dissipated in the localised zone (i.e. the damaged zone), which encompasses deformations associated with the formation and coalescence of distributed longitudinal cracks and deformations at the localised zone (Bažant 1989; Jansen and Shah 1997; Markeset and Hillerborg 1995). In this framework, the total fracture energy (U_{total}) comprises of pre-peak energy (U_{pre}) and post-peak energy (U_{pre}) and it is expressed by the following expression:

$$U_{total} = U_{pre} + U_{post} \qquad (4)$$

Pre-peak energy per unit volume of rock is estimated to be the area under the stress–strain curve enclosed by loading the specimen up to the peak stress and then unloading it completely. The unloading path was assumed to be linear having a slope equal to E_{LVDT} (i.e. the tangent Young's modulus measured by external LVDTs) as shown in Fig. 2a. On the other hand, post-peak energy was

calculated taking into account the area under the post-peak stress-inelastic strain. That is, the area under the unloaded pre-peak stress–strain curve (assuming that unloading curve's Young's modulus, E_{un}, is equal to loading curve's Young's modulus, E_{LVDT}) and under the post-peak stress-inelastic strain as shown in Fig. 2a. Herein, the post-peak fracture energy was defined until a post-peak stress level equal to about one-third of the peak stress, i.e. 0.33 q_{peak}, a stress level where the stress–strain curve is terminated by drawing a linear unloading following a slope equal to E_{LVDT} (Jansen and Edwin 1995; Jansen and Shah 1997). In addition, an elastic energy (U_e) at the peak stress was calculated by the following equation (see Fig. 2b for the notation of U_e).

$$U_e = \frac{UCS^2}{2E_{LVDT}} \tag{5}$$

Different rock types, sourced from different quarries in France, Australia and Iran, including five limestones, a sandstone and two granites, which are presented in Table 1 (UCS is ranging between 7 and 215 MPa), were tested in order to obtain the energies quantities involved during compression in a series of uniaxial compressive tests under quasi-static monotonic loading conditions. The compressive tests complied with the application of a prescribed constant lateral strain-rate of 2×10^{-6}/s as a feedback signal to control the axial load which was found to be a suitable loading rate to measure the complete stress–strain response for the rocks presented in Table 1 as shown in Fig. 2c. Figure 2d shows the relationship of energies quantities U_{total} and U_e with the respective UCS of the studied rocks. This figure shows that U_e clearly increases in a linear fashion with an increase in UCS. The total energy U_{total}, however, increases first and then decreased as UCS increases. This trend complies with low energy enclosed in the stress–strain curve of rocks with higher strength that behave following class I–II or class II behaviour as shown in Fig. 2c. To quantify failure characteristics of different rocks, the following energy-based brittleness index is proposed;

$$B_{U-I} = \frac{U_e}{U_{total}} \tag{6}$$

As can be seen in Fig. 3, unlike a number of brittleness indices including B_1, B_2 and B_3 proposed in previous studies (Altindag 2009, 2010), the proposed brittleness index B_{U-I} is able to describe properly a monotonic and unambiguous scale of brittleness and brittleness relations with increasing rock strength (i.e. UCS). Furthermore, brittleness index B_{U-I} describes a monotonic and unambiguous scale of brittleness with increasing pre-peak strength parameters such as crack damage strength and tangent Young's modulus of rock. This outcome becomes

relevant in order to better understand material brittleness associated with the progressive fracture process characterised by the typical threshold damage stresses and the elasticity parameters. The brittleness index B_{U-I} scale indicates that a higher brittleness index means that rock is more brittle which corresponds to higher strength rocks. From Fig. 3 a non-linear relationship having a coefficient of correlation, R^2, of 0.955 between the brittleness index B_{U-I} and UCS can be established by the following expression:

$$B_{U-I} = 0.563e^{0.0056UCS} \tag{7}$$

The expression above is used to calculate brittleness index of different rocks investigated in this study from their UCS values.

3 PDC Cutting Performance

3.1 Cutting Experiments Conducted in the Present Study

Rock cutting induces either plastic yielding or fracture mode of failure in the rock depending on the depth of cut, d, (Lin and Zhou 2013, 2015; Richard et al. 2012). This is, at relatively shallow depths of cut, plastic yield mode of failure is dominant and material failure is governed by yield strength (i.e. strength-related failure mechanism). On the other hand, when the depth of cut is relatively deep, fracture mode of failure dominates and therefore material failure is governed by its fracture properties (i.e. fracture-related failure mechanism). In these instances, unconfined compressive strength, UCS, and fracture toughness, K, become relevant to characterise plastic yield and fracture mode of failure in cutting, respectively. Lin and Zhou (2013, 2015) demonstrated that rock cutting is well described by Bazant's size effect law (SEL) for quasi-brittle materials, such as concrete and rocks (Bažant 1984). SEL is expressed as a function of the nominal stress $\sigma_N = \left(F_s^C\right)_{peak}/w_c d$ and the depth of cut, d, where $\left(F_s^C\right)_{peak}$ is the peak cutting force and w_c is the cutter width, see Fig. 4 for the geometry and nomenclature of the cutting test.

In this view, a series of cutting experiments using a single polycrystalline diamond compact (PDC) cutter under steady cutting conditions were carried out at depths of cut smaller than 0.5 mm in compliance with plastic yield mode of failure. In doing so, as shown in Table 2, different rock types (UCS is ranging from 9 to 249 MPa) including a limestone (i.e. Tuffeau), three sandstones (i.e. Castlegate, Mountain Gold and Hawkesbury), a phyllite (i.e. Brukunga) and a basalt (i.e. Mantina), which were sourced from several mines and quarries in France and Australia, were used.
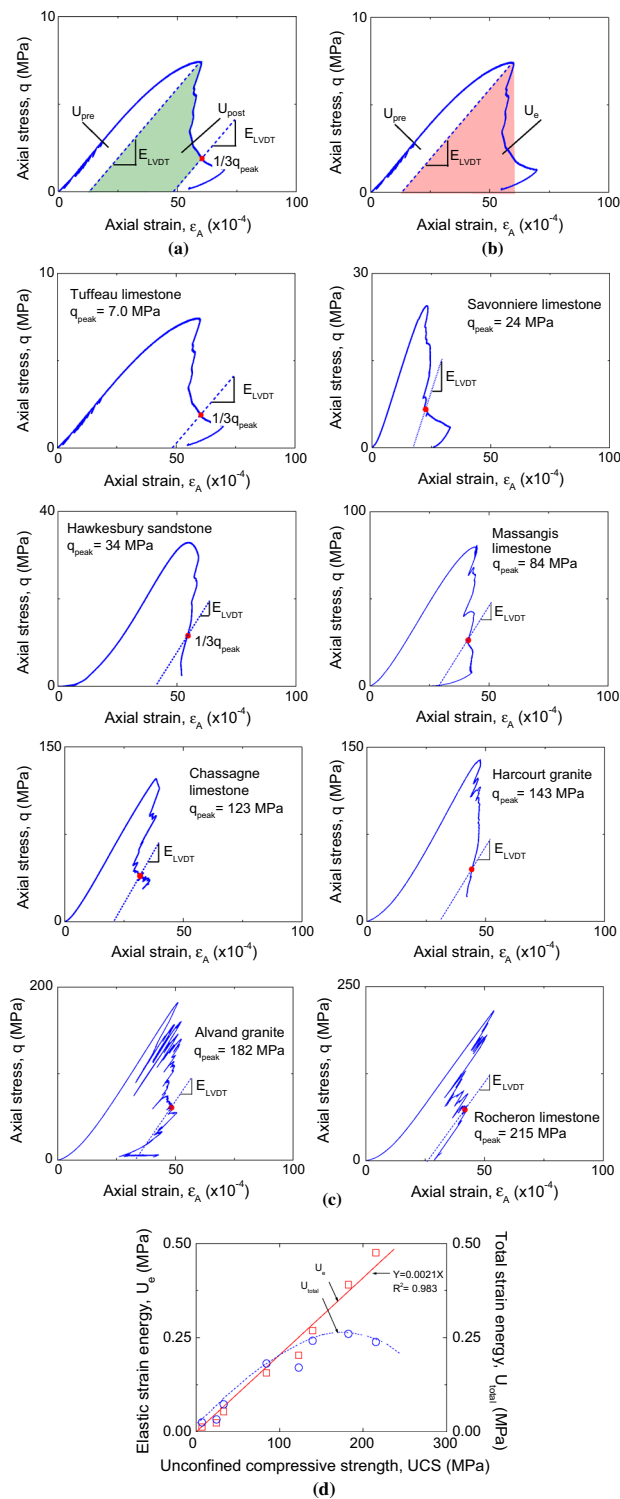
Fig. 2 **a**, **b** Strain energy of rock in compression, **c** typical complete stress–strain curves for different rocks under lateral strain-rate control and **d** strain energy quantities with compressive strength for different rock types

The cutting tests were performed at the Australian Resource Research Centre (ARRC), CSIRO-Perth facilities. The cutting tests were conducted following a standard practice suggested in a previous research (Richard et al. 2012). The cutting device used in the experiment (manufactured by Epslog SA) is equipped with a load sensor which measures the tangential (F_s^C) and normal (F_n^C) components of the cutting force acting on the cutter (see Fig. 4). The cutting machine is controlled by a computer program and the data is stored into a computer by a data acquisition system.

A consistent cut was applied to the surface of the rock samples by means of a rectangular cutter (i.e. a sharp cutter) of width w_c equal to 10 mm. In the tests, the cutter ran along a length of 10 cm under a prescribed constant velocity of 4 mm/s and at a constant depth of cut, d. The rocks were cut at a back-rake angle θ of 15° in all the tests. The depth of cut, d, in the tests varied from 0.1 to 0.5 mm with steps of constant increments of 0.1 mm, in general. The surface of the rocks was carefully prepared by preliminary cuts to achieve an even and smooth surface prior to setting the prescribed depth of cut and start the cutting test. By doing so, it was assured the formation of a groove having constant cross-section area (i.e. a constant $w_c d$) at constant d in each test. Each cutting run was performed strictly over a fresh surface on the rock. Furthermore, the formation of a deep U-type groove due to successive cuts over a same spot was not allowed, so the effect of sidewall friction (cutter-groove), that may cause an additional increase in the intrinsic specific energy spent in cutting the rock (ε) was eliminated (Richard et al. 2010).

3.2 Intrinsic Specific Energy from PDC cutting

The intrinsic specific energy, ε, from PDC cutting can be obtained using the following expression (Richard et al. 2012):

$$\varepsilon = F_s^C / w_c d \tag{8}$$

where, F_s^C represents the average force on steady cutting conditions, d, is the depth of the cut and w_c, represents the cutter width (w_c of 10 mm).

The cutting response of the PDC cutter on the intact rocks presented in Table 2 was characterised by a linear scaling regime between F_s^C and d, as shown in Fig. 5a. The plot between F_s^C and d shows non-zero intercepts in all the tests. This behaviour may be associated to the presence of friction caused by cutter wear (Zhou and Lin 2013). Table 2 summaries the values of intrinsic specific energy (ε) which were obtained from the slope of the linear fitting in the $F_s^C - w_c d$ plot. The values of ε varied from 9 to 220 J/cm^3 for the rocks in Table 2 and they are in good agreement with the magnitude of the UCS of their respective rocks. This result is supporting previous findings by other researchers (Richard et al. 2010, 2012) where the

Table 1 Rocks investigated to develop a energy-based brittleness index B_{U-I}

Rock name	Rock type	UCS (MPa)
Tuffeau	Limestone	7
Savoniere	Limestone	24
Hawksebury	Sandstone	33
Massangis	Limestone	84
Chassagne	Limestone	123
Harcourt	Granite	139
Alvand	Granite	182
Rocheron	Limestone	215
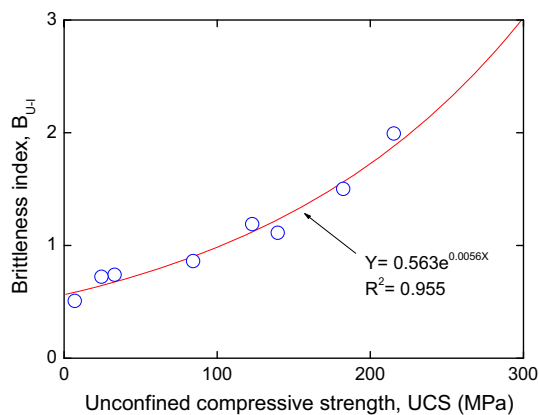
Fig. 3 Brittleness index B_{U-I} relations with unconfined compressive strength for different rock types

intrinsic specific energy increases with an increase in compressive strength. Rock failure governed by plastic yield mode (i.e. strength-related failure mechanism) is demonstrated in Fig. 5b through Bazant's size effect law (SEL) where cutting data at relatively shallow depths of cut, in this case smaller than 0.5 mm, falls into plastic yielding region.

3.3 Intrinsic Specific Energy and Brittleness Index

Figure 6 shows the relationship between the intrinsic specific energy (ε) from the cutting tests and the brittleness index B_{U-I}. The values of B_{U-I} were calculated for the rocks from their respective UCS values as summarised in Table 2 (see the values of UCS and B_{U-I} in Table 2). From this figure, a strong correlation between the intrinsic specific energy and the proposed energy-based brittleness index was found. That is, a correlation coefficient R^2 of 0.999 was yielded by a logarithmic fitting in the form of $\varepsilon = 158LN(B_{I-U}) + 90$.

In Fig. 6, the intrinsic specific energy, which increases with an increase in compressive strength, obviously shows an increasing trend in a non-linear fashion with increasing
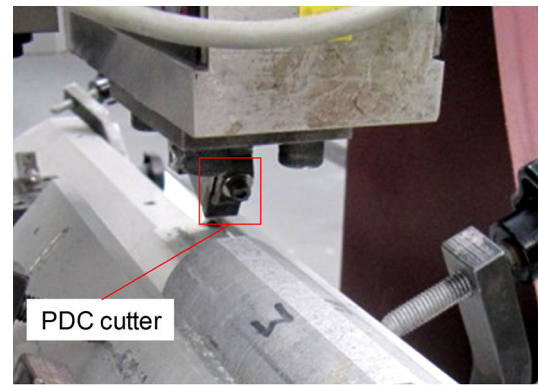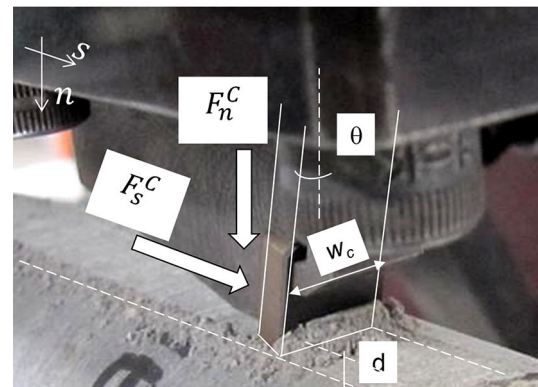
Fig. 4 a PDC cutting test at shallow depth of cut and **b** geometry of cutting and forces acting on the PDC cutter

Table 2 Rocks tested for PDC cutting performance

Rock name	Rock type	UCS (MPa)	ε (MPa)	B_{U-I}
Tuffeau	Limestone	9	9	0.59
Castlegate	Sandstone	16	15	0.62
Mountain Gold	Sandstone	35	26	0.68
Hawksbury	Sandstone	45	42	0.72
Brukunga	Phyllite	103	88	1.00
Mantina	Basalt	249	221	2.27

B_{U-I} as high strength rocks show a higher brittleness capacity by higher B_{U-I} values.

4 Rotary Drilling Performance

4.1 Drilling Experiments from Literature

Independent drilling data found elsewhere in the literature was used to study the relationship between the intrinsic specific energy in drilling with the proposed brittleness index B_{U-I}. In doing so, small-diameter PDC rotary

drilling tests at atmospheric pressure (Stavropoulou 2006) on three marble rocks (i.e. Gioia, Cervaiole and Dionysios) were re-examined to calculate the values of intrinsic specific energy and brittleness index, B_{U-I}. Table 3 lists these rocks and their respective strength parameters. In this case, the small-diameter drilling experiments were conducted using a PDC bit with a diameter of 5 mm with a clearance angle 10°. The back-rake angle θ in the tests was equal to 30°.

In addition, rotary drilling experiments at atmospheric pressure with roller-cone bits (Franca 2010) on two limestones (i.e. Tuffeau and Savonniere) and two sandstones (i.e. Castlegate and Mountain Gold) were re-examined to withdraw the values of intrinsic specific energy from the drilling performance and brittleness index B_{U-I} from rock compressive strength, respectively. Table 4 lists these rocks and their respective strength parameters. In this table, the tensile strength (TS) values for Tuffeau, Savonniere, Castlegate and Mountain Gold were obtained after conducting a series of Brazil tests (Suggested methods for determining tensile strength of rock materials 1978) as part of the present study. The drilling experiments in this case were conducted with an in-house designed drilling rig having a bit assembly consisting of a roller-cone bit (i.e. an insert bit IADC 531 of 2 1/2 and non-insert bit IADC 321 of 2 15/16), a shaft, and a sophisticated anvil.

Finally, additional rotary drilling experiments of roller-cone bits conducted on a sandstone (i.e. Kimachi), an andesite (i.e. Shinkomatsu), and a granite [i.e. Sori (A)] reported by Karasawa et al. (2002a, b) presented in Table 4 were also re-examined. In this case, all the drilling tests were performed at atmospheric pressure using milled-tooth bits (i.e. IADC 221S of 98.4 mm) and insert-tooth bits (i.e. IADC 537X of 101.6 mm). Franca (2010) reports the details and analysis of the experimental data obtained by Karasawa et al. (2002a, b) on the drilling response to obtain the respective intrinsic specific energy.

4.2 Intrinsic Specific Energy from Rotary Drilling

The cutting response of PDC bits, used in a rotary drilling, derives from a combination of two major actions (Detournay and Defourny 1992): (1) a pure cutting action and (2) a frictional action due to the cutter wear-flat area. The energy consumed in a pure cutting action of rock is measured by the intrinsic specific energy (ε) attainable at the cutting point (Detournay and Defourny 1992; Detournay et al. 2008; Franca 2010; Franca et al. 2015). In this instance, drilling efficiency is increased when the energy consumed by the frictional forces are minimised at the optimum weight and torque on the bit to produce the optimum depth of cut. Quantities of consumed energy
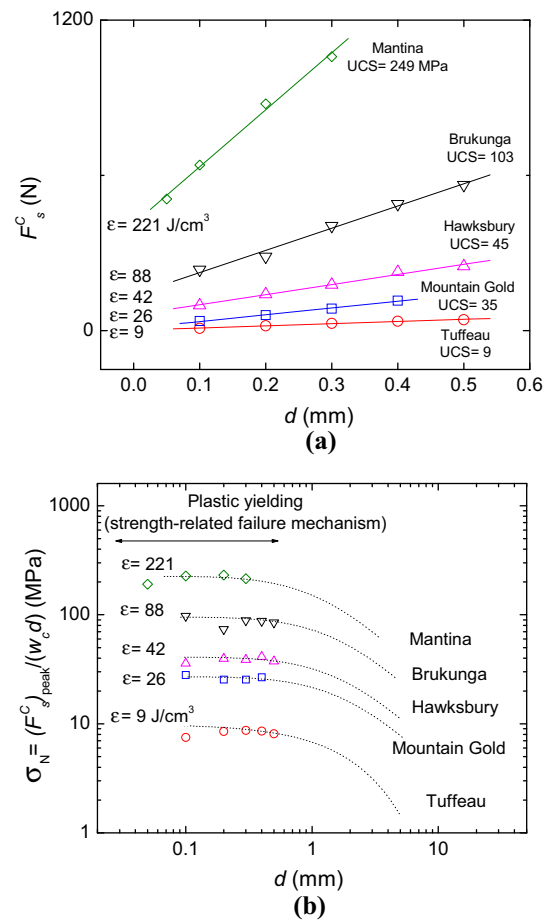

Fig. 5 **a** Cutting force, F_s^C, versus depth of cut, d, **b** SEL for the rock investigated and intrinsic specific energy
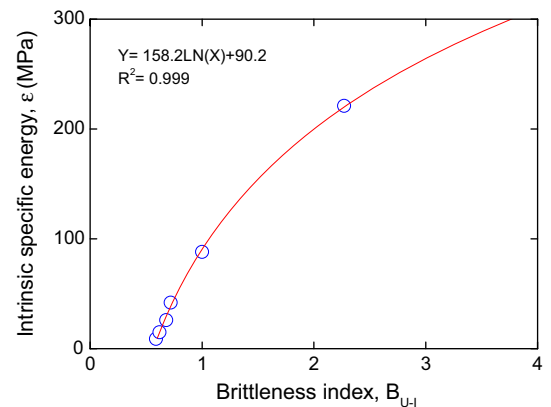

Fig. 6 Intrinsic specific energy from PDC cutting tests and its relation with the brittleness index B_{U-I}

higher than the intrinsic specific energy represent the energy consumed by frictional processes.

The drilling response of PDC drag bits is characterised by a linear relation between weight, torque on the bit and depth of cut per revolution (Detournay and Defourny 1992;

Table 3 Rocks for PDC drilling performance and brittleness index

Rock name[a]	Rock type[a]	UCS (MPa)[a]	TS (MPa)[a]	ε (MPa)[b]	B_{U-I}[b]
Gioia	Marble	101.7	7.5	88	1.00
Cervaiole	Marble	117.1	9.4	125	1.08
Dionysios	Marble	94.2	8.2	103	0.95

[a] Data from literature (Stavropoulou 2006)

[b] Calculated by the authors

Table 4 Rocks for roller-cone drilling performance and brittleness index

Rock name[a,b]	Rock type[a,b]	UCS (MPa)	TS (MPa)	ε (MPa)[a]	B_{U-I}[c]
Tuffeau	Limestone	10[a]	0.86[c]	14	0.60
Savonniere	Limestone	25[a]	2.20[c]	33	0.65
Castlegate	Sandstone	14[a]	1.25[c]	15	0.61
Mountain Gold	Sandstone	26[a]	2.17[c]	32	0.65
Kimachi	Sandstone	45[b]	4.2[b]	42	0.72
Shinkomatsu	Andesite	113[b]	7.7[b]	106	1.06
Sori (A)	Granite	171[b]	10.5[b]	168	1.47

[a] Data from literature (Franca 2010)

[b] Data from literature (Karasawa et al. 2002a, b)

[c] Calculated by the authors

Detournay et al. 2008). Then, the PDC bit response in terms of the Specific Energy is given by the following expression:

$$\text{SE} = \frac{t}{d} = \varepsilon(1 - \mu\tan(\theta + \psi)) + \mu\frac{w}{d} \qquad (9)$$

where SE is the specific energy, t and w are the normalised weight and torque on the bit, respectively, d is the depth of cut per revolution, μ is the coefficient of friction in the wear flat area of a blunt cutter of the bit, and ε is the intrinsic specific energy. Following this approach, the values of intrinsic specific energy for the marble rocks undergoing the small-diameter rotary drilling action in Table 3 were calculated. From Table 3, it can be seen that the values of intrinsic specific energy ε varied from 88 to 125 MPa and are in reasonable agreement with the respective values of UCS of the rocks. This result is supporting previous findings by others (Detournay and Defourny 1992; Detournay et al. 2008) showing that the magnitude of intrinsic specific energy is very similar to the UCS.

The drilling action of roller-cone bits can be considered as a combination of two distinct processes: indentation and cutting actions (Franca 2010). In the case of rotary drilling with roller-cone bits, bit-rock interaction laws are based on the approach initially developed for PDC drag bits as explained above. In this framework, energy dissipation at the bit-rock interaction can be considered as a combination of three independent processes: pure cutting action, pure indentation action, and frictional contact along the wear flat

rock interface (Franca 2010), then the drilling response in this cases is given in terms of the Specific Energy presented as follows:
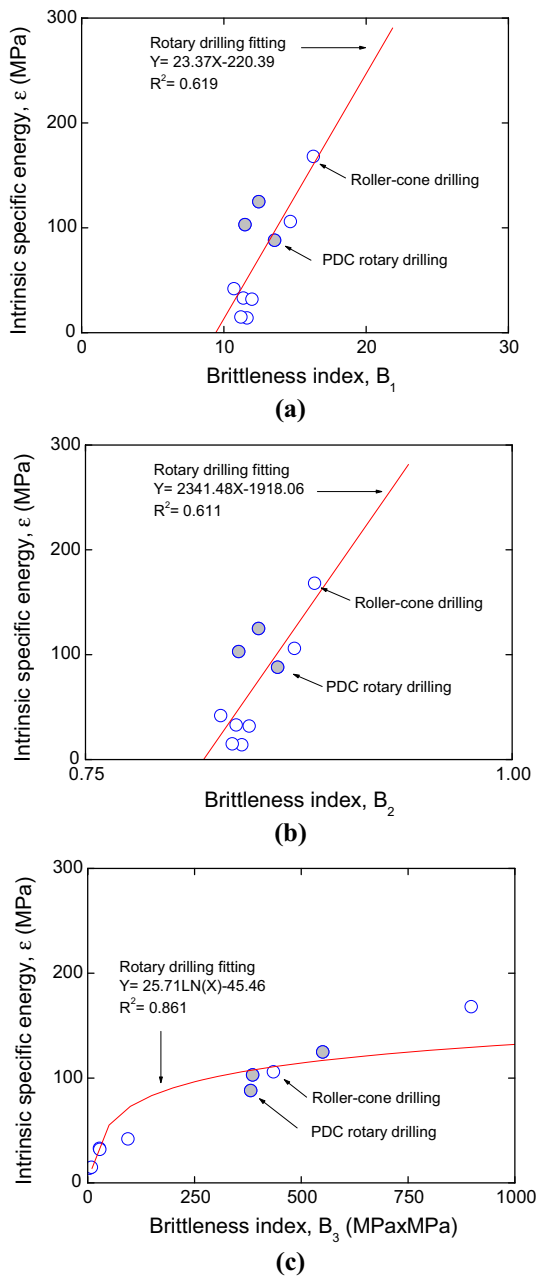
$$\text{SE} = \frac{t}{d} = \varepsilon(1 - \mu\zeta) + \mu\frac{w}{d} \qquad (10)$$

where ζ is a number that characterises the ratio of the cutting-indentation strength to the intrinsic specific energy. Following this approach, Table 4 summarises the intrinsic specific energy values for the limestone and sandstone rocks undergoing roller-cone drilling action obtained by Franca (2010). In addition, this table includes the intrinsic specific energy values obtained from the experimental data reported by Karasawa et al. (2002a, b) on Kimachi sandstone, Shinkomatsu andesite, and Sori (A) granite analysed and reported by Franca (2010). These results are also included in Table 4. From Table 4, it can be seen that the values of intrinsic specific energy ε for these different rock types varied from 14 to 168 MPa and they have values very similar in magnitude to the UCS of their respective rocks.

4.3 Intrinsic Specific Energy and Brittleness Index

Analysis on the correlations of the intrinsic specific energy and other brittleness indices previously proposed to study the drilling performance including B_1, B_2 and B_3, extracted from the data set (i.e. from UCS and TS) presented in Tables 3 and 4, indicates that there is not any notable correlations between the intrinsic specific energy from the drilling experiments with brittleness indices B_1, B_2 and B_3
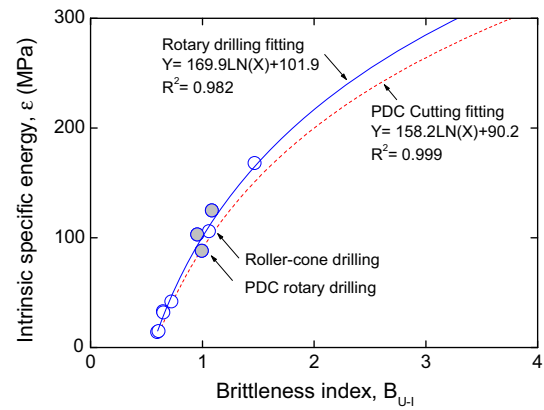
Fig. 7 Intrinsic specific energy and its relation with the brittleness index **a** B_1, **b** B_2 and **c** B_3 from rotary drilling tests

Fig. 8 Intrinsic specific energy from rotary drilling tests and its relation with the brittleness index B_{U-I}

energy from roller-cone rotary drilling and PDC small-diameter rotary drilling and the proposed energy-based brittleness index B_{U-I}. A logarithmic fitting in the form of $\varepsilon = 169LN(B_{I-U}) + 101$, with a coefficient of correlation R^2 of 0.982 were obtained which supports this statement. It is noteworthy that PDC single cutter cutting tests results also lie in a logarithmic fitting curve close to that obtained for the drilling tests results as shown in Fig. 8.

Furthermore, similar to the results with PDC single cutter tests presented earlier, in Fig. 8, the intrinsic specific energy, which increases with increasing compressive strength, obviously increases in a non-linear fashion with B_{U-I} as high strength rocks show a higher brittleness capacity by higher B_{U-I} values.

5 Percussive Drilling Performance

5.1 Drilling Experiments from Literature

In the case of percussive drilling, tool–rock interactions are mostly focused on the prediction of the penetration rate and selection of the optimum thrust (Franca 2011; Hustrulid and Fairhurst 1971a, b, 1972a, b). To examine the application of the proposed brittleness index B_{U-I} in assessing the percussive drilling performance, independent data set from percussive drilling tests carried out in field conditions on a wide variety of rocks with a wide range of uniaxial compressive strength values ranging from 69 to 418 MPa, reported by Schmidt (Schmidt 1972), was used. Here, percussive drilling performance is given in terms of the rate of penetration. Table 5 shows the strength parameters of the rocks and their respective rate of penetration (PR) obtained under bit diameter of 66.68 mm (H-thread carbide bit), operating pressure of 690 kPa, piston weight of 2 kg and air-type flushing.

as shown in Fig. 7. In this view, it is examined in this section whether the new brittleness index B_{U-I} can be reasonably correlated with the drilling parameters obtained from rotary drilling.

Figure 8 shows the relationship between the intrinsic specific energy from Tables 3 and 4 and their respective brittleness index B_{U-I}. Here, B_{U-I} values were calculated from the UCS quantities of the respective rocks and they are presented in Tables 3 and 4. Figure 8 shows that there exists a sound correlation between the intrinsic specific

Table 5 Rocks for percussive drilling performance and brittleness index

Rock type[a]	UCS (MPa)[a]	TS (MPa)[a]	PR (cm/min)[a]	PRN[b] (cm/min)/MPa	B_{U-I}[b]
Iron	418.6	14.6	13.21	0.03	5.87
Schist	208.1	7.5	20.83	0.10	1.8
Pegmatite	89.6	8.6	34.29	0.38	0.93
Quartzite	222.5	17.6	34.8	0.15	1.95
Argillite	220.7	18.4	18.29	0.083	1.93
Dolomite	97.0	4.2	52.32	0.53	0.96
Mankato	125.1	6.4	91.44	0.73	1.13
Quartzite	156.4	15.8	32.51	0.20	1.35
Quartzite	307.2	20.7	21.84	0.07	3.14
Granite	154.6	9.1	26.42	0.17	1.33
Granite	203.5	13.0	22.86	0.11	1.75
Granite	171.1	12.5	31.5	0.18	1.46
Basalt	286.8	28.2	17.02	0.05	2.80
Limestone	99.8	5.7	48.26	0.48	0.98
Taconite	360.9	30.4	21.34	0.05	4.25
Taconite	368.3	22.2	15.49	0.04	4.42
Taconite	364.5	28.8	13.97	0.03	4.33
Diabase	374.7	24.9	21.34	0.05	4.58
Gabbro	208.0	15.1	27.69	0.13	1.80
Trap	68.8	5.1	46.23	0.67	0.82
Anorthosite	131.4	10.5	40.64	0.30	1.17
Basalt	186.3	13.9	33.78	0.18	1.59
Marble	127.5	7.0	38.1	0.29	1.15
Gabbro	176.1	12.7	28.45	0.16	1.50
Iron	225.3	11.8	32.51	0.14	1.98

[a] Data from literature (Schmidt 1972)

[b] Calculated by the authors
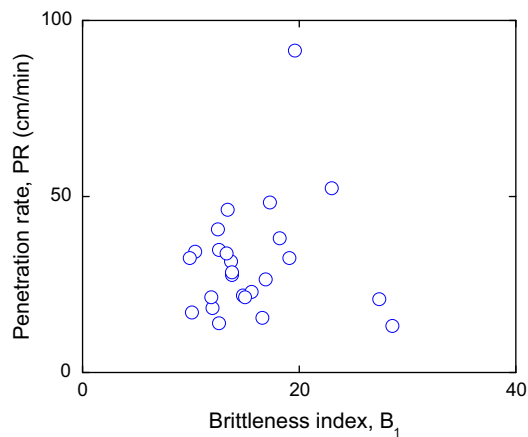
5.2 Penetration Rate and Brittleness Index

In this section, first brittleness indices B_1, B_2 and B_3, proposed in previous studies, and their relations with the penetration rate PR were examined. These brittleness indices were extracted from the data set presented in Table 5 by Schmidt (Schmidt 1972). Results of similar analysis can be found in the literature elsewhere (Altindag 2009). The results of this analysis are presented in Fig. 9. It can be seen in this figure that, B_1 and B_2 show no correlation with the penetration rate. In addition, B_3 does not show a correlation as good as B_{U-I} does with the penetration rate as it is demonstrated later in Fig. 10.

Table 5 reports the values of the brittleness index B_{U-I} calculated from the respective values of UCS of the rocks. Figure 10a shows the plot penetration rate PR versus the brittleness index B_{U-I}. This figure shows that there is a reasonable correlation between the penetration rate PR and the proposed energy-based brittleness index B_{U-I}. This correlation is stronger than others presented in Fig. 9. An

exponential fitting in the form of $PR = 39.49B_{U-I}^{-0.59}$ which yielded a coefficient of correlation R^2 of 0.753. In Fig. 10a, in general, the penetration capacity given by the penetration rate of the rocks decreases non-linearly with an increase in brittleness index B_{U-I} (i.e. with an increase in compressive strength of the rocks). This is mainly because penetration rate in stronger rocks drops and stronger rocks have higher B_{U-I} values.

In order to improve the correlation between penetration rate PR and B_{U-I} data, the penetration rate values were normalised with respect to the uniaxial compressive strength, i.e. by dividing the penetration rate by the respective UCS of rocks producing the normalised penetration rate PRN = PR/UCS. This normalisation has also been proposed and used in previous studies on the application of brittleness index to predict drilling performance (Altindag 2009, 2010).
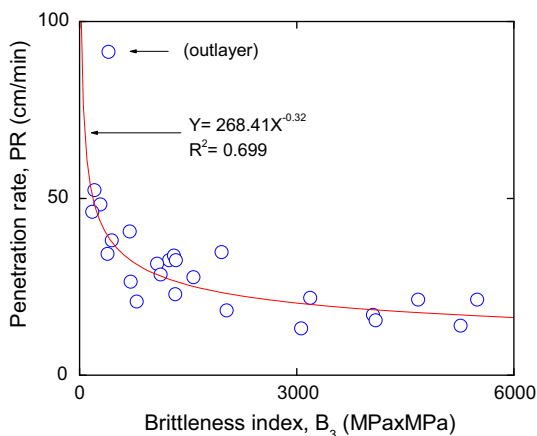
The results of normalisation show that the normalised penetration rate values PRN decreases non-linearly as the brittleness B_{U-I} increases and a correlation
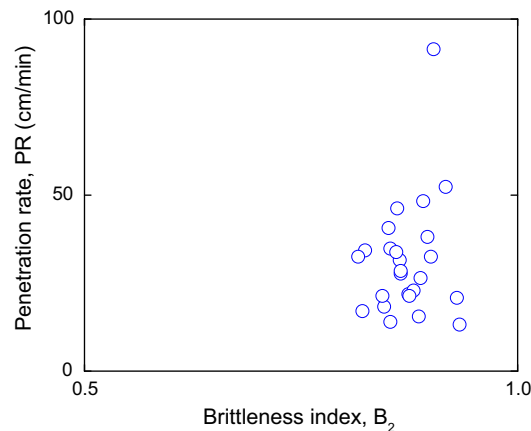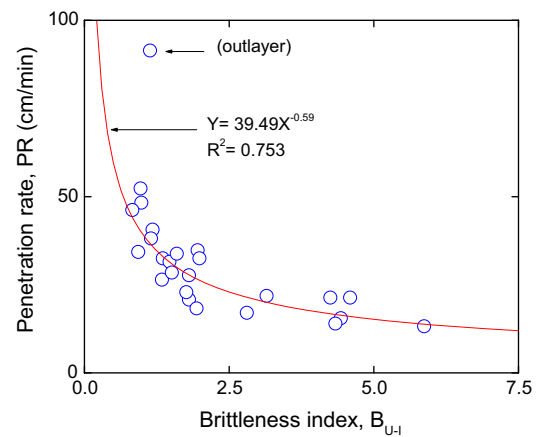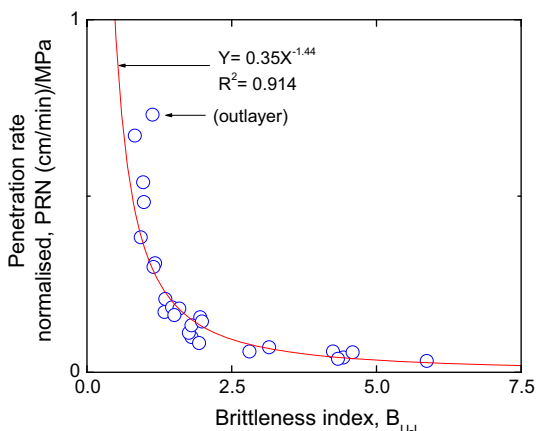
Fig. 9 Penetration rate and its relation with the brittleness index **a** B_1, **b** B_2 and **c** B_3 from percussive drilling tests

coefficient R^2 of 0.914 was yielded with an exponential fitting of $PRN = 0.35B_{U-I}^{-1.44}$. Brittleness indices B_1, B_2 and B_3 and their relations with the penetration rate normalised PRN were also examined (results are not shown here). In this respect, B_1 and B_2 were not able to produce any correlation and B_3 did not show a

Fig. 10 a Penetration rate and **b** penetration rate normalised from percussive drilling tests and their relation with the brittleness index B_{U-I}

correlation as good as B_{U-I} did with the normalised penetration rate data.

6 Conclusions

In this study drilling performance is evaluated by rock brittleness capacity. In this respect, to reliably estimate drilling performance both tool–rock interaction laws along with a proper brittleness index should be implemented. Therefore, tool–rock interaction laws together with a new brittleness index able to picture both an ambiguous brittleness scale from ductile to brittle and brittleness scale with rock strength were implemented. This new brittleness index B_{U-I}, which is based on the relation of the energy dissipation quantities withdrawn from the complete stress–strain curve in uniaxial compression, was deemed to be relevant to this purpose.

The performance of PDC single-cutter cutting tests and different drilling methods including PDC rotary drilling,

roller-cone rotary drilling and percussive drilling were investigated against rock brittleness capacity. PDC single-cutter cutting experiments were carried out on different rock types. In addition, independent rotary as well as percussive drilling results from laboratory and field tests, found in the literature, were used. To quantify cutting and drilling performance, the intrinsic specific energy, which is the energy consumed in pure cutting action, and drilling penetration rate values were implemented. The results show that the new energy-based brittleness index B_{U-I} successfully describes the performance of the studied cutting and drilling methods.

In addition, the performance of several brittleness indices which are proposed based on relations between compressive and tensile strength, i.e. B_1, B_2 and B_3, were investigated and compared with the proposed brittleness index B_{U-I}. These brittleness indices, however, are not able to quantify rock failure behaviour and cannot correlate well with rock strength. As a result, no correlation was found between brittleness B_1 and B_2 with either cutting or drilling performance parameters. Brittleness index, B_3 showed some correlation with drilling performance parameters, however, in all drilling cases, B_3 showed weaker correlations with drilling performance parameters as compared to the correlations obtained by B_{U-I}. The brittleness index, B_{U-I} proposed in the present study offered the strongest correlation with the drilling performance, either case cutting, rotary or percussive drilling. Therefore, the new energy-based brittleness index is deemed to be relevant to assess drilling performance by rock brittleness capacity.

References

Altindag R (2002) The evaluation of rock brittleness concept on rotary blast hole drills. J S Afr Inst Min Metall 102:61–66

Altindag R (2003) Correlation of specific energy with rock brittleness concepts on rock cutting. J S Afr Inst Min Metall 103:163–171

Altindag R (2009) Assessment of some brittleness indexes in rock-drilling efficiency. Rock Mech Rock Eng 43:361–370. doi:10.1007/s00603-009-0057-x

Altindag R (2010) Reply to the discussion by Yagiz on "Assessment of some brittleness indexes in rock-drilling efficiency" by Altindag. Rock Mech Rock Eng 43:375–376. doi:10.1007/s00603-009-0057-x

Bažant Z (1984) Size effect in blunt fracture: concrete. Rock Metall J Eng Mech 110:518–535. doi:10.1061/(ASCE)0733-9399(1984)110:4(518)

Bažant Z (1989) Identification of strain softening constitutive relation from uniaxial tests by series coupling model for localisation. Cem Concr Res 19:973–997

Detournay E, Atkinson C (2000) Influence of pore pressure on the drilling response in low-permeability shear-dilatant rocks. Int J Rock Mech Min Sci 37:1091–1101. doi:10.1016/S1365-1609(00)00050-2

Detournay E, Defourny P (1992) A phenomenological model for the drilling action of drag bits. Int J Rock Mech Min Sci Geomech Abstr 29:13–23. doi:10.1016/0148-9062(92)91041-3

Detournay E, Richard T, Shepherd M (2008) Drilling response of drag bits: theory and experiment. Int J Rock Mech Min Sci 45:1347–1360. doi:10.1016/j.ijrmms.2008.01.010

Franca LFP (2010) Drilling action of roller-cone bits: modeling and experimental validation. J Energy Res Technol 132:043101. doi:10.1115/1.4003168

Franca LFP (2011) A bit–rock interaction model for rotary–percussive drilling. Int J Rock Mech Min Sci 48:827–835. doi:10.1016/j.ijrmms.2011.05.007

Franca LFP, Mostofi M, Richard T (2015) Interface laws for impregnated diamond tools for a given state of wear. Int J Rock Mech Min Sci 73:184–193. doi:10.1016/j.ijrmms.2014.09.010

Hoseinie SH, Aghababaei H, Pourrahimian Y (2008) Development of a new classification system for assessing of rock mass drillability index (RDi). Int J Rock Mech Min Sci 45:1–10. doi:10.1016/j.ijrmms.2007.04.001

Howarth D (1987) The effect of pre-existing microcavities on mechanical rock performance in sedimentary and crystalline rocks. Int J Rock Mech Min Sci and Geomech Abstr 4:223–233 (Elsevier)

Hucka V, Das B (1974) Brittleness determination of rocks by different methods. Int J Rock Mech Min Sci Geomech Abstr 11:389–392. doi:10.1016/0148-9062(74)91109-7

Hustrulid W, Fairhurst C (1971a) A theoretical and experimental study of the percussive drilling of rock part II—force-penetration and specific energy determinations. Int J Rock Mech Min Sci Geomech Abstr 4:335–356 (Elsevier)

Hustrulid WA, Fairhurst C (1971b) A theoretical and experimental study of the percussive drilling of rock part I—theory of percussive drilling. Int J Rock Mech Min Sci Geomech Abstr 8:311–333. doi:10.1016/0148-9062(71)90045-3

Hustrulid W, Fairhurst C (1972a) A theoretical and experimental study of the percussive drilling of rock part III—experimental verification of the mathematical theory. Int J Rock Mech Min Sci Geomech Abstr 3:417–418 (Elsevier)

Hustrulid WA, Fairhurst C (1972b) A theoretical and experimental study of the percussive drilling of rock part IV—application of the model to actual percussion drilling. Int J Rock Mech Min Sci Geomech Abstr 9:431–442. doi:10.1016/0148-9062(72)90007-1

International Society for Rock Mechanics, Commission on Standardization of Laboratory and Field Tests, Commmittee on Laboratory Tests (1978) Suggested methods for determining tensile strength of rock materials. Int J Rock Mech Min Sci Geomech Abstr 15:99–103. doi:10.1016/0148-9062(78)90003-7

Jansen DC, Edwin CR (1995) Stress–strain results of concrete from circumferential strain feedback control testing. Mater J 92:419–428. doi:10.14359/9774

Jansen DC, Shah S (1997) Effect of length on compressive strain softening of concrete. J Eng Mech 123:25–35. doi:10.1061/(ASCE)0733-9399(1997)123:1(25)

Kahraman S (1999) Rotary and percussive drilling prediction using regression analysis. Int J Rock Mech Min Sci 36:981–989. doi:10.1016/S0148-9062(99)00050-9

Kahraman S (2002) Correlation of TBM and drilling machine performances with rock brittleness. Eng Geol 65:269–283. doi:10.1016/S0013-7952(01)00137-5

Kahraman S, Balcı C, Yazıcı S, Bilgin N (2000) Prediction of the penetration rate of rotary blast hole drills using a new drillability index. Int J Rock Mech Min Sci 37:729–743. doi:10.1016/S1365-1609(00)00007-1

Kahraman S, Bilgin N, Feridunoglu C (2003) Dominant rock properties affecting the penetration rate of percussive drills. Int J Rock Mech Min Sci 40:711–723. doi:10.1016/S1365-1609(03)00063-7

Karasawa H, Ohno T, Kosugi M, Rowley JC (2002a) Methods to estimate the rock strength and tooth wear while drilling with roller-bits—part 1: milled-tooth bits. J Energy Res Technol 124:125. doi:10.1115/1.1482405

Karasawa H, Ohno T, Kosugi M, Rowley JC (2002b) Methods to estimate the rock strength and tooth wear while drilling with roller-bits—part 2: insert bits. J Energy Res Technol 124:133. doi:10.1115/1.1482406

Kidybiński A (1981) Bursting liability indices of coal. Int J Rock Mech Min Sci Geomech Abstr 18:295–304. doi:10.1016/0148-9062(81)91194-3

Lin J-S, Zhou Y (2013) Can scratch tests give fracture toughness? Eng Fract Mech 109:161–168. doi:10.1016/j.engfracmech.2013.06.002

Lin J-S, Zhou Y (2015) Rebuttal: shallow wide groove scratch tests do not give fracture toughness. Eng Fract Mech 133:211–222. doi:10.1016/j.engfracmech.2014.10.030

Markeset G, Hillerborg A (1995) Softening of concrete in compression—localization and size effects. Cem Concr Res 25:702–708. doi:10.1016/0008-8846(95)00059-L

Munoz H, Taheri A, Chanda E (2016) Fracture energy-based brittleness index development and brittleness quantification by pre-peak strength parameters in rock uniaxial compression. Rock Mech Rock Eng (submitted)

Paone J, Madson D, Bruce WE (1969) Drillability studies: laboratory percussive drilling. Bureau of Mines, Twin Cities Mining Research Center, Twin Cities

Richard T, Coudyzer C, Desmentte S (2010) Influence of groove geometry and cutter inclination in rock cutting. Paper presented at the 44th US rock mechanics symposium and 5th US-Canada rock mechanics symposium, Salt Lake City, UT, USA

Richard T, Dagrain F, Poyol E, Detournay E (2012) Rock strength determination from scratch tests. Eng Geol 147–148:91–100. doi:10.1016/j.enggeo.2012.07.011

Schmidt RL (1972) Drillability studies: percussive drilling in the field. Report of investigations 7684, 31 P, 1972 11 Fig, 10 Tab, 11 Ref

Selim AA, Bruce WE (1970) Prediction of penetration rate for percussive drilling. Report of investigations 7396, June, 1970 21 P, 13 Tab, 10 Ref, Append

Stavropoulou M (2006) Modeling of small-diameter rotary drilling tests on marbles. Int J Rock Mech Min Sci 43:1034–1051. doi:10.1016/j.ijrmms.2006.03.008

Taheri A, Qao Q, Chanda E (2016) Drilling penetration rate estimation using rock drillability characterization index. J Inst Eng (India) Ser D. doi:10.1007/s40033-015-0104-6

Tarasov B, Potvin Y (2013) Universal criteria for rock brittleness estimation under triaxial compression. Int J Rock Mech Min Sci 59:57–69. doi:10.1016/j.ijrmms.2012.12.011

Tarasov BG, Randolph MF (2011) Superbrittleness of rocks and earthquake activity. Int J Rock Mech Min Sci 48:888–898. doi:10.1016/j.ijrmms.2011.06.013

Teale R (1965) The concept of specific energy in rock drilling. Int J Rock Mech Min Sci 2:57–73

Zhou Y, Lin J-S (2013) On the critical failure mode transition depth for rock cutting. Int J Rock Mech Min Sci 62:131–137. doi:10.1016/j.ijrmms.2013.05.004